Title

Diffusion tensor imaging during recovery from severe traumatic brain injury and relation to clinical outcome: a longitudinal study.

Journal

Brain : a journal of neurology, 131(Pt 2)

ISSN

0006-8950

Authors

Sidaros, Annette
Engberg, Aase W
Sidaros, Karam
et al.

Publication Date

2008-02-01

DOI

10.1093/brain/awm294

Peer reviewed

doi:10.1093/brain/awm294 *Brain* (2008), **131**, 559–572

Diffusion tensor imaging during recovery from severe traumatic brain injury and relation to clinical outcome: a longitudinal study

Annette Sidaros,[1,2] Aase W. Engberg,[2] Karam Sidaros,[1] Matthew G. Liptrot,[1] Margrethe Herning,[1] Palle Petersen,[3] Olaf B. Paulson,[1,4] Terry L. Jernigan[1,5] and Egill Rostrup[1]

[1]Danish Research Centre for Magnetic Resonance, Copenhagen University Hospital, Hvidovre, Denmark, [2]Brain Injury Unit, Department of Neurorehabilitation, Copenhagen University Hospital, Hvidovre, Denmark, [3]Department of Neurology, Copenhagen University Hospital, Rigshospitalet, Denmark, [4]Neurobiology Research Unit, Copenhagen University Hospital, Rigshospitalet, Denmark and [5]Laboratory of Cognitive Imaging, Department of Psychiatry, University of California, San Diego, CA, USA

Correspondence to: Annette Sidaros (previously Annette S. Nielsen), MD, Danish Research Centre for Magnetic Resonance, Copenhagen University Hospital, Hvidovre, Department 340, 2650 Hvidovre, Denmark
E-mail: annettes@drcmr.dk

Diffusion tensor imaging (DTI) has been proposed as a sensitive biomarker of traumatic white matter injury, which could potentially serve as a tool for prognostic assessment and for studying microstructural changes during recovery from traumatic brain injury (TBI). However, there is a lack of longitudinal studies on TBI that follow DTI changes over time and correlate findings with long-term clinical outcome. We performed a prospective longitudinal study of 30 adult patients admitted for subacute rehabilitation following severe traumatic brain injury. DTI and conventional MRI were acquired at mean 8 weeks (5–11 weeks), and repeated in 23 of the patients at mean 12 months (9–15 months) post-trauma. Using a region-of-interest-based approach, DTI parameters were compared to those of healthy matched controls, scanned during the same time period and rescanned with a similar interval as that of patients. At the initial scan, fractional anisotropy was reduced in all the investigated white matter regions in patients compared to controls ($P \leqslant 0.01$) due to decreased diffusivity parallel ($\lambda_{\parallel}$) and increased diffusivity perpendicular ($\lambda_{\perp}$) to axonal fibre direction. Fractional anisotropy in the cerebral peduncle correlated with ~1 year Glasgow outcome scale score ($r = 0.60$, $P < 0.001$) and in this sample predicted dichotomized outcome with 76% accuracy when taken alone, and with 100% accuracy in combination with clinical evaluation by functional independence measure at the time of the first scan. At follow-up DTI, fractional anisotropy in patients had increased in the internal capsule and in centrum semiovale ($P \leqslant 0.01$) due to an interval increase of $\lambda_{\parallel}$ with unchanged $\lambda_{\perp}$. In these regions, fractional anisotropy and $\lambda_{\parallel}$ reached normal or supranormal levels, primarily in patients with favourable outcome. In the cerebral peduncle and in corpus callosum, $\lambda_{\parallel}$ and $\lambda_{\perp}$ both increased during the scan interval and, particularly in patients with unfavourable outcome, fractional anisotropy remained depressed. No significant DTI parameter changes over time were found in controls, or in CSF of patients. These findings support that DTI is a clinically relevant biomarker in TBI, which may have prognostic value and also might serve as a tool for revealing changes in the neural tissue during recovery.

Keywords: diffusion tensor imaging (DTI); traumatic brain injury (TBI); magnetic resonance imaging (MRI); outcome prediction; neuroplasticity

Abbreviations: CP = cerebral peduncle; CSO = centrum semiovale; DAI = diffuse axonal injury; DTI = diffusion tensor imaging; FA = fractional anisotropy; FLAIR = fluid-attenuated inversion recovery; FIM = functional independence measure; GCS = Glasgow coma scale; GOS = Glasgow outcome scale; ISS = injury severity score; MD = mean diffusivity; PCC = posterior aspect of corpus callosum; PLIC = posterior limb of internal capsule; PTA = post-traumatic amnesia; PUT = putamen; ROIs = regions of interest; TBI = traumatic brain injury

Received May 20, 2007. Revised November 6, 2007. Accepted November 7, 2007. Advance Access publication December 14, 2007

Introduction

Traumatic brain injury (TBI) is a major cause of death and severe disability under the age of 45 years in Western countries (MacKenzie, 2000). Diffuse-type (non-focal) injuries are generally the most devastating, yet their assessment *in vivo* is hampered by the low sensitivity of conventional imaging. The key mechanism of primary injury is diffuse axonal injury (DAI), which results from rotational acceleration–deceleration causing shear strain deformation and subsequent disconnection of axons. DAI is characterized by microscopic lesions scattered throughout the white matter, with the parasagittal white matter, corpus callosum and the dorsolateral upper brainstem being most commonly involved. Secondary hypoxic-ischaemic injury due to, e.g. insults of hypotension, hypoxia and/or increased intracranial pressure, is known to markedly worsen prognosis following TBI (see e.g. Chesnut *et al.*, 1993). With time both of these diffuse-type injuries lead to Wallerian-like degeneration of white matter (Graham and Gennarelli, 1997).

Recently, much interest has been directed towards the potential of diffusion tensor imaging (DTI) as a tool for *in vivo* quantification of white matter microstructural alterations following TBI (see e.g. Schiff, 2006). DTI is a relatively new MRI modality that non-invasively provides information regarding the degree and directionality of tissue water diffusion (Basser *et al.*, 1994). This technique describes the diffusion process using three eigenvectors, of which the magnitudes, the eigenvalues (λ_1, λ_2, λ_3), quantify the diffusion in three orthogonal directions. Due to barriers to water diffusion imposed by e.g. myelin and membranes, hindrance of diffusion is larger across than along axonal fibres, causing diffusion in white matter to be anisotropic. Anisotropy is commonly expressed relative to the magnitude of the diffusion tensor as the fractional anisotropy (FA) (Pierpaoli and Basser, 1996), and this index ranging from 0 to 1 is found to be higher in intact white matter consisting of highly parallel fibres. Mean diffusivity (MD), or 'apparent diffusion coefficient', refers to the average of the three eigenvalues. While commonly only these summary parameters, FA and MD, are reported, the underlying eigenvalues hold additional valuable information as they may be selectively affected with certain pathological processes (Song *et al.*, 2002).

In a recent experimental study, correlations between DTI and histology of DAI were demonstrated (Mac Donald *et al.*, 2007). Prior clinical DTI-studies on TBI have found reduced FA in several white matter areas, both within lesions and in tissue appearing normal on conventional MRI (Rugg-Gunn *et al.*, 2001; Arfanakis *et al.*, 2002; Chan *et al.*, 2003; Ptak *et al.*, 2003; Huisman *et al.*, 2004; Inglese *et al.*, 2005; Salmond *et al.*, 2006; Nakayama *et al.*, 2006). At post-acute stages, MD in areas of decreased FA has been found to be normal or increased (Rugg-Gunn *et al.*, 2001; Chan *et al.*, 2003; Inglese *et al.*, 2005; Salmond *et al.*, 2006; Nakayama *et al.*, 2006). The eigenvalues were reported in one of the aforementioned studies of five patients with mild TBI (Arfanakis *et al.*, 2002) and in one case study (Le *et al.*, 2005), suggesting that decrease of the major eigenvalue, λ_1, and increase of the minor eigenvalues λ_2 and λ_3 may underlie FA (and MD) alterations. Some association has been reported between DTI values (in splenium and internal capsule) and short-term outcome (Huisman *et al.*, 2004). However, as most prior studies were cross-sectional, few investigated correlations of DTI with long-term (>6 months) clinical outcome. Moreover, little is known about the long-term evolution of diffusion abnormalities during recovery from TBI. Apart from reports on one or two patients (Arfanakis *et al.*, 2002; Naganawa *et al.*, 2004; Le *et al.*, 2005; Voss *et al.*, 2006), longitudinal DTI studies in TBI have not, to our knowledge, been published previously. DTI repeated during rehabilitation and correlated with long-term clinical outcome may add to our understanding of the natural course of diffuse traumatic injuries and of the mechanisms of neuroplasticity and repair operating during recovery from TBI.

We performed a prospective longitudinal study of 30 patients with severe TBI, comparing results to 30 healthy matched controls. With the current study we sought to examine the correlation between white matter DTI measures in the late subacute (or early chronic) phase and 1-year clinical outcome, and to investigate whether DTI repeated about 1 year post-trauma would detect white matter microstructural alterations. Additionally, we wished to determine which diffusivity changes underlie FA (and MD) abnormalities in severe TBI. We hypothesized that, for one or more of the investigated white matter areas, (i) FA would be reduced in TBI patients in the late subacute phase, (ii) FA would increase in patients during the scan interval, (iii) FA would deviate more from control values, at both scan time points, in patients with poorer long-term clinical outcome.

Material and Methods

Subjects

The study was approved by the local Scientific Ethics Committee (KF 01-038/03). Informed consent was obtained from the participants or from next of kin, meeting criteria of the Helsinki Declaration.

Thirty adult patients (age 18–65 years, mean 34 years; 23 males, 7 females) with severe TBI were recruited from the Brain Injury Unit at Copenhagen University Hospital Hvidovre, Denmark, to which they were admitted for subacute rehabilitation between 2003 and 2005. Severe TBI was defined as a post-resuscitation Glasgow Coma Scale (GCS; Teasdale and Jennett, 1974) score $\leqslant 8$ measured within 24 h post-injury and prior to the initiation of paralytics or sedatives. Patients were referred from neuro-intensive units, and admitted for rehabilitation only if they had subnormal GCS after cessation of sedation. All adult patients with severe TBI admitted during the recruitment period were evaluated for study eligibility. Patients were excluded if they had any previous history of TBI or other neurological disorder, if contraindications to MRI or to sedation

Table 1 Clinical characteristics of patients

Patient	Age at scan 1 (years)	Sex	Cause of trauma	Post-resuscitation GCS	Neuro-surgery	ISS	Secondary insults	Days to GCS > 8	Duration of PTA (days)	FIM at scan 1	FIM at 1 year	GOS at 1 year
1	19	M	MVA	4	–	35	+	10	>FU	29	83	3
2	23	F	MVA	3	–	43	+	36	79	47	120	3
3[a]	23	F	Fall	3	–	45	+	>FU	>FU	18	18	2
4[a]	21	F	MVA	6	+	25	–	12	39	79	117	3
5[a]	34	M	MVA	3	–	66	+	126	>FU	18	30	3
6[a]	40	F	Fall	3	+	25	+	9	>FU	18	20	3
7[a]	40	M	Assault	3	–	29	+	4	88	87	122	4
8[a]	60	M	Fall	3	+	25	–	21	>FU	34	35	3
9[a]	28	M	MVA	NA	–	34	–	24	66	122	125	5
10	54	M	Fall	NA	–	25	–	14	119	60	125	4
11[a]	26	M	MVA	3	–	35	–	2	25	110	126	5
12[a]	24	M	MVA	3	–	26	–	1	39	93	125	4
13[a]	65	M	Fall	3	–	29	–	3	39	116	120	4
14[a]	31	M	MVA	5	+	25	+	7	48	38	102	4
15[a]	37	M	MVA	NA	+	38	–	14	40	117	122	5
16[a]	22	M	MVA	NA	–	43	–	7	31	120	125	5
17[a]	19	M	MVA	6	–	33	–	2	23	113	124	5
18[a]	41	F	MVA	6	+	34	–	10	65	55	113	4
19[a]	26	M	MVA	6	–	25	+	22	65	106	124	4
20	60	M	Fall	3	–	26	+	18	289	31	30	3
21[a]	22	M	MVA	3	–	43	+	9	178	18	103	3
22	61	M	Fall	5	+	25	+	22	>FU	18	25	3
23[a]	23	M	MVA	3	–	25	+	11	107	23	111	3
24[a]	18	F	MVA	3	–	29	+	15	66	24	105	3
25[a, b]	40	M	Fall	3	+	25	–	10	84	100	117	4
26[a]	53	M	Fall	4	+	25	+	5	171	18	111	4
27	28	M	Fall	3	–	38	+	15	180	18	36	3
28	31	M	MVA	3	–	38	+	33	>FU	18	22	3
29[a]	27	M	MVA	6	–	45	+	10	77	49	113	4
30[a]	26	F	MVA	7	–	29	–	4	58	59	126	5

[a]Patients who had follow-up DTI; [b]excluded from DTI analysis (acquisition error). MVA = motor vehicle accident; GCS = Glasgow coma scale; NA = not available (GCS $\leqslant$ 8 but exact GCS not documented); > FU = exceeds ~1 year follow-up; ISS = injury severity score (> 25 indicates extra-cranial injury); PTA = post-traumatic amnesia; FIM = functional independence measure; Scan 1 = initial MRI; GOS = Glasgow outcome scale. See text for details.

during MRI were present, or if MRI could not be performed within 12 weeks post-trauma for safety or practical reasons.

After discharge, patients were re-admitted for clinical follow-up on average 12 months (9–15 months) post-injury (one patient who moved far away was instead visited and evaluated in his home by the treating physician). During, or as close as possible, to this stay a second scan was obtained in 23 of the patients. For the remaining patients follow-up DTI could not be acquired due to: relocation ($n = 1$), inability to complete the repeat examination because of poor cooperation ($n = 4$), insertion of MRI-incompatible implants ($n = 1$), or scanner failure ($n = 1$). Table 1 summarizes clinical data for the patients studied.

Thirty healthy controls, without any history of significant TBI or neurological disorder, were selected to match the patient group with respect to distribution of age, sex, educational level and abuse of alcohol and drugs (Table 2). Of these, 14 were investigated longitudinally with a time interval comparable to that of the patients.

Clinical assessments

For all patients, clinical data and ratings were documented in medical files. Cause of trauma was classified as motor vehicle accident ($n = 19$), fall ($n = 10$) or assault ($n = 1$). Accidents with any direct involvement of a motor vehicle (including pedestrian or bicyclist hit by car) were classified as motor vehicle accident. GCS was registered frequently in the acute phase and daily during rehabilitation, only to be discontinued if stable at 15. As an indicator of the total injury severity to all organ systems, Injury Severity Score (ISS, Greenspan *et al.*, 1985) was assessed based on clinical data from the acute phase (ISS >25 indicates extracranial injury). Secondary insults were defined as the occurrence of any of the following in the acute or subacute phase: hypotension (systolic blood pressure <90 mmHg), hypoxia (oxygen saturation <90% or cyanosis in field) or high intracranial pressure (ICP >20 mmHg) (Jones *et al.*, 1994). Neurosurgery was defined as surgery that involved craniotomy, excluding insertion of ICP monitoring devices.

The number of days from TBI until GCS >8 was registered as a measure of coma duration, and the Galveston Orientation and Amnesia Test (Levin *et al.*, 1979) was repeatedly applied to establish duration of post-traumatic amnesia (PTA). Functional Independence Measure (FIM; Granger *et al.*, 1986) was documented regularly, including at both scan time points (sum score ranges from 18 indicating 'total assist', to 126 indicating 'complete independence'). Functional outcome at ~12 months post-TBI was

Table 2 Demographic characteristics of patient and control groups

	Scan 1			Scan 2		
	Patients ($n = 30$)	Controls ($n = 30$)	Group differences	Patients ($n = 23$)	Controls ($n = 14$)	Group differences
Age, scan 1 (years), mean (SD)	34.1 (14.3)	34.0 (13.9)	$P > 0.99$[a]	32.4 (12.9)	31.2 (8.1)	$P > 0.7$[a]
Sex: M/F	23/7	23/7	$P = 1.0$[b]	17/6	9/5	$P > 0.7$[b]
Education (years), mean (SD)	13.3 (3.1)	13.4 (2.3)	$P > 0.99$[a]	13.4 (3.1)	13.7 (2.7)	$P > 0.7$[a]
Excessive alcohol intake (> 21 drinks per week for men, > 14 for women), Y/N	5/25	4/26	$P = 1.0$[b]	4/19	0/14	$P = 0.3$[b]
Use of drugs (cannabinoids or psycho-stimulants) > once a month, Y/N	3/27	1/29	$P > 0.6$[b]	3/20	0/14	$P = 0.3$[b]

[a]Independent-samples *t*-test; [b]Fishers exact test. Scan 1 = initial MRI; Scan 2 = follow-up MRI.

evaluated using the 5-point Glasgow Outcome Scale (GOS; Jennett and Bond, 1975), ranging from 1 = dead to 5 = good recovery. Based on previous literature (see e.g. Choi *et al.*, 2002), GOS = 1–3 was considered as unfavourable outcome and GOS = 4–5 as favourable outcome, thus distinguishing whether or not patients were able to live independently. All clinical ratings were performed by trained staff, neurologists and neuropsychologists unaware of DTI results.

MRI data acquisition

MRI including DTI was acquired 5–11 weeks (mean 8 weeks) after trauma. A more uniform time interval was not achievable, mainly because patients had to be medically stable when scanned. All patients were referred to conventional MRI for clinical purposes. DTI and other sequences not reported here were performed as an extension of the MRI examination. The majority of patients ($n = 25$) were sedated for the initial MRI, since they were unable to cooperate for MRI. Intravenously administered propofol was used for sedation, and patients were monitored by anaesthesiology staff. Oxygen supply and mechanical ventilation were provided when necessary.

All patients and controls were scanned on the same 1.5 T MRI scanner (Magnetom Vision; Siemens Medical Solutions, Erlangen, Germany) using a standard circular-polarized head coil. During the study period, MRI sessions for patients and controls were interleaved in time, and no major upgrades were carried out on the scanner. A 3D sagittal T1-weighted sequence (TR/TE/TI = 13.5/7/100 ms, flip angle 15°, spatial resolution of $\sim$1 mm^3) was acquired in all subjects. For patients, additional conventional sequences included: axial T2-weighted images (spin-echo, TR/TE = 5400/99 ms, 27 contiguous, 5 mm thick slices, 0.5 × 0.5 mm^2 in-plane resolution), coronal T2*-weighted gradient-echo images (TR/TE = 544/15 ms, 34 contiguous, 5 mm thick slices, 0.9 × 0.9 mm^2 in-plane resolution), axial and sagittal FLAIR (TR/TE/TI = 9000/110/2500 ms, 34 contiguous, 5 mm thick slices, 0.9 × 0.9 mm^2 in-plane resolution).

All subjects underwent DTI using a diffusion-weighted spin-echo single-shot echo-planar imaging (EPI) sequence acquired with diffusion encoding in 6 non-collinear directions and averaged over six datasets for a total acquisition time of $\sim$15 min. The sequence parameters were as follows: TE = 60 ms, field of view 230 mm, matrix 128 × 128, 30 axial slices, 5 mm slice thickness, b values 0 and $\sim$740 s/mm^2 with diffusion sensitizing gradient pulses of duration = 29 ms (δ) and separation = 52 ms (Δ).

Follow-up MRI was acquired in 23 of the patients (9–15 months post-injury, mean 12 months), and in 14 of the controls. A minimum of DTI and 3D T1-weighted images were obtained at follow-up with the parameters described earlier. Subjects were repositioned as close as possible to their position in the previous scan. For ethical reasons patients were sedated only if follow-up MRI was requested for clinical purposes and patients were unable to cooperate for MRI because of cognitive impairment. While 19 patients were fully cooperative, four were sedated for the follow-up MRI. Four patients were not sufficiently cooperative to complete the follow-up MRI but could not be sedated.

For one patient, careful inspection of the diffusion-weighted images acquired at the initial scan revealed an abnormally low signal-to-noise ratio (most likely due to miscalibration of the radio-frequency transmitter reference). We therefore excluded DTI data for this patient (initial and follow-up scan) from statistical analysis.

MRI data analysis

Evaluation of conventional MRI

The conventional images were qualitatively evaluated for all patients by an experienced neuroradiologist (M.H.) blinded to the DTI findings and clinical ratings. This evaluation included classification of all visible lesions based on their signal characteristics (see e.g. Gentry, 2002). Additional careful inspection of the regions of interest (ROIs) was done subsequently.

Regions of interest

Images were transferred to an offline workstation for post-processing, and were visually checked for quality. All ROIs were outlined manually on spatially normalized 3D T1-weighted structural images (Fig. 1). Spatial normalisation of the T1-weighted images according to the MNI template was performed using a 12 parameter transformation in SPM2 (http://www.fil.ion.ucl.ac.uk/spm). Using image display software (MIPAV, version 2.0, http://mipav.cit.nih.gov) the following white matter ROIs were positioned for each individual scan: posterior aspect of the corpus callosum (PCC), posterior limb of internal capsule (PLIC), centrum semiovale (CSO) and cerebral peduncle (CP). Additional ROIs in ventricular CSF and in the putamen (PUT), expected to be relatively unaffected by TBI, served as internal references for MD. In order to minimize misregistration stemming from

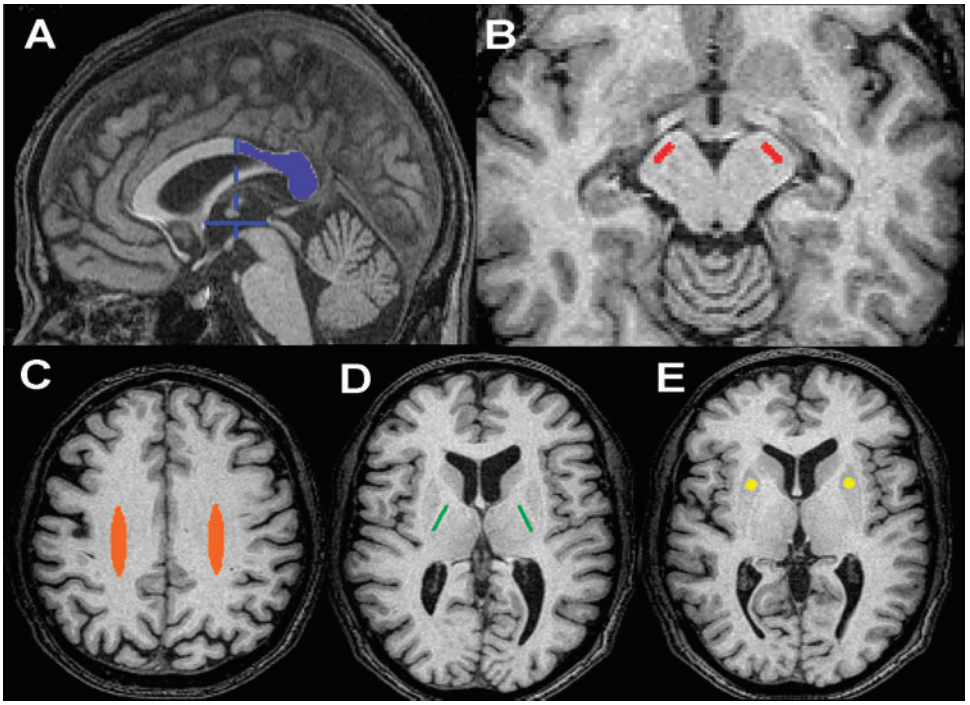

Fig. 1 ROIs used in the study. ROIs were drawn on normalized 3D T1-W images (shown) for each individual scan. (**A**) Posterior aspect of corpus callosum (PCC). Anterior border is defined by midpoint of the AC–PC line; (**B**) cerebral peduncle (CP); (**C**) centrum semiovale (CSO); (**D**) posterior limb of internal capsule (PLIC); (**E**) putamen (PUT). See text for details.

EPI-related susceptibility artifacts, we avoided ROIs in the most frontal cerebral areas. As structural changes were expected to occur over time, ROIs were redrawn/repositioned for all follow-up scans to ensure identical anatomical positioning for initial and follow-up scans. ROIs were positioned by anatomic guidance, not lesion guidance, and were outlined bilaterally in the axial plane, except for PCC which was outlined in the sagittal plane. For statistical analysis, bilateral measurements were averaged.

The PCC ROI [volume (mean ± SD) = 2513 ± 479 µl] was drawn according to the callosal borders on the midsagittal slice plus the four adjacent parasagittal slices on each side, with the anterior border being defined arbitrarily by a line perpendicularly crossing the midpoint of the anterior-posterior commissural (AC–PC) line. Anatomically, the PCC included the splenium, isthmus and posterior part of the body of corpus callosum. The PLIC (171 ± 2 µl) was sampled by a rectangle in the centre of the structure on the four axial slices where it appeared broadest. For the CSO (4820 ± 46 µl) an ellipse was placed centrally in the hemispherical white matter on 8–10 axial slices. The CP (150 ± 0 µl) was sampled by a polygonal ROI on five slices of the upper mesencephalon. For reference (MD only), a circular ROI was placed in the centre of the PUT (672 ± 0 µl), transversing 10–12 axial slices and ventricular CSF was sampled on one axial slice (43 ± 5 µl).

Except for the PCC, the borders of the ROIs were kept distant from adjacent tissue/CSF. For PCC a step-wise erosion algorithm, with each step eroding the exterior voxel layer in the sagittal plane, was subsequently applied to test for possible partial volume effects, i.e. the unintentional inclusion in the ROIs of other than the tissue of interest. Due to global atrophy during the scan interval, the volumes of some ROIs (particularly the PCC) were smaller at the follow-up scan in many patients.

All ROIs were outlined by the same rater (A.S.). For evaluation of intra-rater reproducibility, ROIs were positioned 3 times (with evaluations separated by 1–2 days) in four subjects (two controls, two patients). Between-scan reproducibility was estimated using additional data from three healthy subjects scanned twice with a maximum interval of 4 weeks.

Every individual ROI was inspected carefully for lesions visible on conventional sequences (T1, T2, T2*, FLAIR). Since DAI lesions were often punctate and multiple we did not attempt to eliminate DAI lesions from the ROIs. Instead, individual ROIs were excluded from statistical analysis (both initial and follow-up) only if they contained non-DAI lesions. If one ROI was excluded, the contralateral one was used for analysis (bilateral ROIs).

DTI post-processing

Diffusion-weighted images were coregistered to the $b = 0$ images using a 12 parameter algorithm in SPM2. The six repetitions for each measured direction were averaged to increase the signal-to-noise ratio. The diffusion tensor (D) and its eigenvalues (λ_1, λ_2, λ_3) and eigenvectors were then estimated for each voxel (Basser *et al.*, 1994), the calculations being performed in native space prior to spatial normalization. By sorting the eigenvalues in order of decreasing magnitude for each voxel ($\lambda_1 > \lambda_2 > \lambda_3$), λ_1 represents the diffusivity along the primary diffusion direction, i.e. along the fibre axis, and is referred to as the *axial* diffusivity, $\lambda_{\|}$. The averaged water diffusivities perpendicular to the axonal fibres, λ_2 and λ_3, are referred to as $\lambda_{\perp} = (\lambda_2 + \lambda_3)/2$, or the *radial* diffusivity (Song *et al.*, 2002). The summary parameters MD and FA were calculated voxel-wise according to (Pierpaoli and Basser, 1996).

Coregistration and extraction of DTI values

For each scan the $b=0$ images were coregistered to the corresponding spatially normalized 3D structural T1-weighted images using normalized mutual information. This transformation was then applied to the calculated diffusion parameter maps and these were resliced using tri-linear interpolation in SPM2. For all scans coregistration was visually checked by superimposing the images (including the ROIs). The coregistration was done after calculating the diffusion parameters in order to avoid any effects this spatial normalization step might have on the calculation of the diffusion tensor. The only effect the normalization has on the diffusion parameter maps is therefore a slight smoothing due to the reslicing. Following coregistration, diffusion parameters (FA, MD, $\lambda_{\parallel}$ and $\lambda_{\perp}$) were extracted from each ROI and summarized as the median value of the voxels comprising the ROI.

For those subjects who had a follow-up scan, a pairwise coregistration of the second to the first 3D T1-weighted volume was performed, followed by the normalization applied in the first scan. The calculated diffusion images were then coregistered to the T1-weighted images as described earlier.

Statistical analysis

Statistical analyses were performed with SPSS (v.15.0), and the threshold for statistical significance was set at $P<0.05$. Shapiro–Wilk's test was used to test the distribution of DTI parameters, and since deviation from normality was not found parametric statistics were applied. For measures of intra-rater and between-scan reproducibility, the coefficient of variation (CV) was computed (CV = SD/mean). To test the principal hypotheses, independent-samples *t*-tests (two-tailed) were conducted to compare FA between patients and controls as well as between favourable and unfavourable outcome subgroups, while paired *t*-tests (two-sided) were used to examine changes over time. Bonferroni correction for multiple comparisons was made for tests of the principal hypotheses regarding FA (four white matter ROIs were tested, hence $P<0.0125$ was considered significant following correction).

To further examine the basis of any FA differences, we conducted secondary comparisons on the additional diffusion parameters MD, $\lambda_{\parallel}$ and $\lambda_{\perp}$. Additional secondary analyses of clinical and conventional imaging variables relative to dichotomized outcome were performed using independent-samples *t*-test (continuous normally distributed variables), Mann–Whitney U-test (continuous non-normally distributed variables) and Fisher's exact test (categorical variables). Finally, we employed a binary logistic regression analysis (forward step-wise, likelihood ratio) to determine the ability of DTI at the initial scan (~8 weeks post-trauma) to predict dichotomized ~1-year outcome, and to assess the added value of DTI compared to prediction of outcome by clinical evaluation (FIM) only.

Results

Conventional MRI

All but one patient exhibited signal abnormalities consistent with DAI on one or more conventional sequences, presenting as pettechial haemorrhages on T2*-weighted images and/or hyperintensities on FLAIR within typical locations. These abnormalities however ranged from a few subtle lesions identified in a single anatomic location to multiple clear and widespread lesions. Graded according to location (Graham and Gennarelli, 1997), 5 patients had visible DAI lesions confined to the hemispheres (grade I), 15 had visible DAI lesions in the corpus callosum but not in the brainstem (grade II) and 9 had additional DAI-related lesions in the brainstem (grade III).

Residual lesions other than DAI were found on conventional MRI in 26 of 30 patients (initial scan); frequently several types of lesions coexisted. The following intracranial abnormalities were found (number of patients): cortical contusion(s) (15), small subdural haematoma (7), intracerebral haematoma (3), arterial dissection (1), abscess (1), territorial arterial infarction (4), focal brainstem infarct (1), diffuse hypoxic injury (1) and pyramidal tract degeneration in the brainstem (4). Individual ROIs containing non-DAI lesions on conventional MRI and therefore excluded from statistical analysis were: one left PLIC, one left CSO, two right CSO, one left CP, one right CP, one left PUT and two right PUT. Controls all had unremarkable T1-weighted images within and outside ROIs.

At follow-up general atrophy was pronounced in many patients, notably ventricular size had increased and callosal thickness decreased compared to the initial MRI. In many patients the pyramidal tract in the brainstem exhibited bilateral degenerative abnormalities at follow-up.

DTI

Reproducibility of DTI measures was satisfactory for all white matter ROIs, regarding both intra-rater (CV $\leqslant$3% for FA) and between-scan (CV $\leqslant$4% for FA) measurements. As expected, in areas of low anisotropy (PUT and CSF), variation of FA was much higher (intra-rater CV up to 26%, between-scan CV up to 19%), whereas MD showed good reproducibility (intra-rater CV $\leqslant$2%, between-scan CV <3%).

Table 3 lists DTI results for the initial and follow-up scans of the patients (mean 8 weeks and 12 months post-injury) as compared to the controls. DTI values in controls were in the same range as those reported previously (e.g. Pierpaoli *et al.*, 1996; Marenco *et al.*, 2006). At the initial scan, FA was found to be significantly decreased in all white matter ROIs (PCC, PLIC, CSO, CP) in patients as compared with controls ($P<0.000001$ for PCC and CP, $P\leqslant 0.01$ for PLIC and CSO). These results remained significant following Bonferroni correction. Except for CP, MD in patients was not significantly different from controls at the initial scan. Investigating the underlying axial ($\lambda_{\parallel}$) and radial ($\lambda_{\perp}$) diffusivities, for PCC, PLIC and CP this revealed significantly decreased $\lambda_{\parallel}$ ($P<0.00001$ for PCC, $P<0.001$ for PLIC, $P<0.000001$ for CP) as well as increased $\lambda_{\perp}$ ($P<0.0001$ for PCC, $P<0.05$ for PLIC, $P<0.001$ for CP). Hence, decrease of FA was caused by the combined effects of $\lambda_{\parallel}$ decrease and $\lambda_{\perp}$ increase. MD was relatively unaffected as these effects counterbalanced.

Table 3 Diffusion parameters, mean (SD) for each ROI, initial and follow-up scans

		FA		MD [$\times 10^{-3}$mm^2/s]		$\lambda_{\parallel}$ [$\times 10^{-3}$mm^2/s]		$\lambda_{\perp}$ [$\times 10^{-3}$mm^2/s]	
ROI	Scan	Controls	Patients	Controls	Patients	Controls	Patients	Controls	Patients
PCC	1	0.55 (0.06)	**0.42 (0.08)*****	1.08 (0.10)	1.10 (0.07)	1.85 (0.14)	1.67 (0.12)***	0.72 (0.11)	0.84 (0.10)***
	2	0.57 (0.06)	**0.37 (0.08)*****	1.06 (0.09)	1.27 (0.11)***	1.85 (0.10)	1.80 (0.13)	0.68 (0.11)	1.02 (0.14)***
PLIC	1	0.68 (0.05)	**0.64 (0.06)****	0.80 (0.06)	0.80 (0.05)	1.55 (0.07)	1.48 (0.09)***	0.43 (0.07)	0.46 (0.06)*
	2	0.69 (0.05)	0.67 (0.05)	0.79 (0.05)	0.84 (0.07)**	1.53 (0.08)	1.59 (0.08)*	0.41 (0.07)	0.46 (0.08)
CSO	1	0.39 (0.08)	**0.35 (0.06)****	0.88 (0.08)	0.89 (0.08)	1.28 (0.09)	1.24 (0.10)	0.68 (0.11)	0.71 (0.08)
	2	0.40 (0.08)	0.39 (0.08)	0.87 (0.07)	0.92 (0.09)	1.27 (0.12)	1.33 (0.10)	0.67 (0.09)	0.71 (0.11)
CP	1	0.70 (0.03)	**0.60 (0.07)*****	0.84 (0.06)	0.80 (0.07)*	1.66 (0.09)	1.41 (0.15)***	0.43 (0.06)	0.50 (0.07)***
	2	0.72 (0.03)	**0.59 (0.07)*****	0.80 (0.07)	0.90 (0.10)***	1.62 (0.10)	1.58 (0.13)	0.40 (0.05)	0.57 (0.11)***
PUT	1	0.21 (0.04)	0.23 (0.07)	0.79 (0.07)	0.80 (0.05)	0.95 (0.08)	0.99 (0.09)	0.71 (0.06)	0.71 (0.05)
	2	0.20 (0.03)	0.26 (0.05)***	0.78 (0.05)	0.82 (0.07)	0.93 (0.05)	1.03 (0.11)**	0.71 (0.05)	0.71 (0.06)
CSF	1	0.13 (0.05)	0.12 (0.04)	3.21 (0.11)	3.20 (0.12)	3.63 (0.19)	3.61 (0.25)	2.98 (0.11)	2.98 (0.08)
	2	0.12 (0.04)	0.12 (0.07)	3.20 (0.19)	3.22 (0.18)	3.59 (0.31)	3.64 (0.38)	3.00 (0.15)	3.00 (0.14)

Initial scan (scan 1): $n = 29$ patients, 30 controls; follow-up Initial scan (scan 2): $n = 22$ patients, 14 controls $^{*}P < 0.05$ $^{**}P \leqslant 0.01$ $^{***}P \leqslant 0.001$ (uncorrected), independent-samples *t*-tests, patients compared with controls. For principal analyses (FA in white matter ROIs), bold values indicate that patients remained significantly different from controls following Bonferroni correction ($P < 0.0125$). Secondary analyses (MD, $\lambda_{\parallel}$, $\lambda_{\perp}$) are displayed on the right; reference ROIs for MD (PUT and CSF) at the bottom (shaded). PCC = posterior aspect of corpus callosum; PLIC = posterior limb of internal capsule; CSO = centrum semiovale; CP = cerebral peduncle; PUT = putamen; CSF = cerebrospinal fluid; FA = fractional anisotropy; MD = mean diffusivity; $\lambda_{\parallel}$ = axial diffusivity; $\lambda_{\perp}$ = radial diffusivity.

Table 4 Longitudinal DTI findings in 22 patients, mean (SD)

	FA		MD [$\times 10^{-3}$mm^2/s]		$\lambda_{\parallel}$ [$\times 10^{-3}$mm^2/s]		$\lambda_{\perp}$ [$\times 10^{-3}$mm^2/s]	
ROI	Scan 1	Scan 2	Scan 1	Scan 2	Scan 1	Scan 2	Scan 1	Scan 2
PCC	0.42 (0.07)	**0.37 (0.08)*****	1.10 (0.07)	1.27 (0.11)***	1.66 (0.11)	1.80 (0.13)***	0.84 (0.09)	1.02 (0.14)***
PLIC	0.64 (0.05)	**0.67 (0.05)****	0.79 (0.05)	0.84 (0.07)***	1.47 (0.10)	1.59 (0.08)***	0.46 (0.06)	0.46 (0.08)
CSO	0.35 (0.07)	**0.39 (0.08)****	0.88 (0.08)	0.92 (0.09)*	1.24 (0.11)	1.33 (0.10)***	0.71 (0.08)	0.71 (0.11)
CP	0.61 (0.07)	0.59 (0.07)*	0.80 (0.07)	0.90 (0.10)***	1.42 (0.16)	1.58 (0.13)***	0.49 (0.07)	0.57 (0.11)***
PUT	0.22 (0.07)	0.26 (0.05)**	0.79 (0.05)	0.82 (0.07)	0.97 (0.08)	1.03 (0.11)**	0.70 (0.05)	0.71 (0.06)
CSF	0.11 (0.04)	0.12 (0.07)	3.19 (0.13)	3.22 (0.18)	3.62 (0.24)	3.64 (0.38)	2.99 (0.11)	3.00 (0.14)

$^{*}P < 0.05$; $^{**}P \leqslant 0.01$; $^{***}P \leqslant 0.001$ (uncorrected), paired *t*-tests. For principal analyses (FA in white matter ROIs), bold values indicate that results remained significant following Bonferroni correction ($P < 0.0125$). Secondary analyses (MD, $\lambda_{\parallel}$, $\lambda_{\perp}$) are displayed on the right; reference ROIs for MD (PUT and CSF) at the bottom (shaded). Scan 1 = initial MRI; Scan 2 = follow-up MRI; PCC = posterior aspect of corpus callosum; PLIC = posterior limb of internal capsule; CSO = centrum semiovale; CP = cerebral peduncle; PUT = putamen; CSF = cerebrospinal fluid; FA = fractional anisotropy; MD = mean diffusivity; $\lambda_{\parallel}$ = axial diffusivity; $\lambda_{\perp}$ = radial diffusivity.

For the CSO, $\lambda_{\parallel}$ and $\lambda_{\perp}$ were not significantly different from controls ($P > 0.1$). MD was not significantly different between patients and controls in the grey matter ROI (PUT) or in CSF ($P > 0.4$). For these reference ROIs FA, $\lambda_{\parallel}$ and $\lambda_{\perp}$ are listed for completeness.

The DTI changes over time are further presented in Table 4 for the 22 patients who were rescanned ~12 months post-injury. During the scan interval FA increased in PLIC and CSO ($P \leqslant 0.01$). However in PCC, FA decreased further ($P < 0.0001$). These findings remained significant following Bonferroni correction. Investigating the changes of the underlying eigenvalues revealed that $\lambda_{\parallel}$ increased in all white matter ROIs ($P < 0.00001$ for PCC, $P < 0.000001$ for PLIC, $P < 0.0001$ for CSO and CP). In PCC and CP this was accompanied by significant increase of $\lambda_{\perp}$ ($P < 0.000001$ for PCC, $P < 0.001$ for CP), i.e. all eigenvalues changed in the same direction and consequently large increases of MD were seen in these ROIs ($P < 0.000001$ for PCC, $P < 0.0001$ for CP). However, in PLIC and CSO, $\lambda_{\perp}$ did not change over time, and so the observed FA (and MD) increase was caused by a selective $\lambda_{\parallel}$ increase in these ROIs. For each ROI the direction of change in each DTI parameter was the same in almost all patients individually. However, in a few cases values were unchanged or went slightly in the opposite direction.

In CSF no significant changes over time were seen. In PUT however, an unexpected increase of FA over time was found ($P < 0.01$). Computing FA in isotropic or nearly isotropic areas, such as in CSF and PUT, is subject to considerable noise (cf. the poor reproducibility in these areas), which makes it difficult to interpret this latter finding.

Controls had comparable DTI parameter values at the initial and follow-up scans in all ROIs, with no trends of any systematic effects over time. Additional testing of change over

Table 5 Erosion of PCC, effect on DTI metrics, initial and follow-up scans, mean (SD)

		FA		MD [$\times 10^{-3}$mm^2/s]		$\lambda_{\|}$ [$\times 10^{-3}$mm^2/s]		$\lambda_{\perp}$ [$\times 10^{-3}$mm^2/s]	
	Scan	Controls	Patients	Controls	Patients	Controls	Patients	Controls	Patients
0 erosions	1	0.55 (0.06)	**0.42 (0.08)*****	1.08 (0.10)	1.10 (0.07)	1.85 (0.14)	1.67 (0.12)***	0.72 (0.11)	0.84 (0.10)***
	2	0.57 (0.06)	**0.37 (0.08)*****	1.06 (0.09)	1.27 (0.11)***	1.85 (0.10)	1.80 (0.13)	0.68 (0.11)	1.02 (0.14)***
1 erosion	1	0.61 (0.06)	**0.48 (0.08)*****	1.00 (0.08)	1.03 (0.07)	1.83 (0.14)	1.64 (0.13)***	0.60 (0.10)	0.74 (0.10)***
	2	0.64 (0.05)	**0.43 (0.08)*****	0.98 (0.08)	1.17 (0.11)***	1.83 (0.10)	1.74 (0.15)*	0.57 (0.09)	0.89 (0.14)***
2 erosions	1	0.67 (0.06)	**0.54 (0.09)*****	0.93 (0.07)	0.96 (0.06)	1.80 (0.14)	1.61 (0.15)***	0.50 (0.09)	0.64 (0.10)***
	2	0.69 (0.05)	**0.50 (0.09)*****	0.92 (0.07)	1.07 (0.10)***	1.82 (0.11)	1.70 (0.16)**	0.48 (0.08)	0.76 (0.13)***
3 erosions	1	0.70 (0.06)	**0.58 (0.09)*****	0.90 (0.07)	0.91 (0.07)	1.80 (0.14)	1.59 (0.17)***	0.45 (0.09)	0.57 (0.10)***
	2	0.72 (0.05)	**0.54 (0.09)*****	0.88 (0.07)	1.01 (0.10)***	1.82 (0.11)	1.68 (0.18)**	0.42 (0.08)	0.68 (0.12)***

Initial scan (scan 1): $n = 29$ patients, 30 controls; follow-up scan (scan 2): $n = 22$ patients, 14 controls. $^{*}P < 0.05$ $^{**}P \leqslant 0.01$ $^{***}P \leqslant 0.001$ (uncorrected), independent-samples *t*-tests, patients compared to controls. For principal analyses (FA), bold values indicate that patients remained significantly different from controls following Bonferroni correction ($P < 0.0125$). PCC = posterior aspect of corpus callosum; FA = fractional anisotropy; MD = mean diffusivity; $\lambda_{\|}$ = axial diffusivity; $\lambda_{\perp}$ = radial diffusivity.

time in patients compared to change over time in controls (independent-samples *t*-test, data not shown) therefore yielded statistical differences comparable to those in Table 4.

As DAI lesions visible on conventional MRI were frequently present within PCC, supplemental analysis was made for the subgroup of patients without any visible abnormalities in PCC on conventional MRI ($n = 6$, corresponding to DAI grade I or no DAI). For this subgroup FA was still significantly lower in PCC compared to the controls, both at the initial scan and at follow-up ($P < 0.02$).

To test and correct for partial volume effects of the PCC, a step-wise (up to 3 times) erosion of the exterior voxel layer of PCC was performed in the sagittal plane. As displayed in Table 5, this could indicate partial voluming of the uneroded ROI (FA increased, while MD, $\lambda_{\perp}$ and, to a lesser extent, $\lambda_{\|}$ decreased with each erosion step). However, when repeating statistical analysis on the eroded PCC, differences between patients and controls remained significant, even after three erosions.

Volumes of the PCC ROI in patients were generally smaller at follow-up compared to the initial scan (mean 2.1 versus 2.5 ml, $P < 0.00001$, paired *t*-test), since in most patients callosal thinning occurred during the scan interval. As this could introduce systematic differences in partial voluming, the longitudinal analysis was repeated using the eroded PCC (data not shown). Changes over time in patients remained significant following three erosions for all DTI parameters ($P < 0.01$, paired *t*-tests).

Potential influence of the occurrence of secondary insults on DTI parameters was examined, and although FA values in some ROIs appeared to be more depressed in patients with secondary insults, this did not approach significance. Additionally, careful data inspection revealed no trends towards the influence of sedation upon DTI parameters.

Clinical outcome correlations

Table 6 summarizes statistical analysis on demographic, clinical and conventional imaging variables when comparing patients according to dichotomized ~1-year outcome (favourable: GOS = 4–5, corresponding to good recovery or moderate disability; unfavourable: GOS = 1–3, corresponding to severe disability, vegetative state or death). Clinical features significantly related to outcome were post-resuscitation GCS, occurrence of secondary insults, duration of coma, duration of PTA and FIM (measured at the time of the initial MRI). Presence of DAI grade III, as based on conventional MRI, just yielded significance as being associated with unfavourable outcome. The occurrence of focal contusions on conventional MRI was not significantly different between outcome groups.

Figure 2 illustrates the DTI findings at ~8 weeks post-TBI in relation to dichotomized 1-year outcome, with control values shown for comparison. There was a general tendency for patients with unfavourable outcome to deviate more from control DTI values than patients with favourable outcome, not only for FA but also for the underlying diffusivities. Following Bonferroni correction FA in CP remained significantly different between outcome groups. Further examination of the relationship between FA in CP and 1-year GOS revealed significant correlations, with higher FA being related to higher GOS ($r = 0.60$, $P < 0.001$, Spearman's correlation), see Fig. 3.

When FA in CP was included in a logistic regression model to predict dichotomized 1-year outcome, a moderately good predictive accuracy was found (76%, $\chi^2 = 15.6$, $P < 0.0001$). Not surprisingly, FIM measured at the time of the initial scan (~8 weeks post-injury) also had a high predictive accuracy (90%, $\chi^2 = 19.6$, $P < 0.00001$). However, adding FA in CP to a model containing FIM yielded a significantly improved predictive accuracy (increment $\chi^2 = 20.5$, $P < 0.00001$), which in this sample reached 100%. In comparison, conventional MRI variables (e.g. DAI grade) did not improve the predictive accuracy of FIM in a logistic regression model. Neither did FA in white matter ROIs other than CP.

Figure 4 displays the results analogous to Fig. 2 for the follow-up DTI ~12 months post-trauma. In the favourable

Table 6 Significance of demographic, clinical and conventional imaging variables relative to ~1 year outcome

	~1 year outcome (dichotomized GOS)		
	Favourable ($n = 16$)	Unfavourable ($n = 14$)	P
Age, years (mean ± SD)	34.9 ± 13.1	33.1 ± 15.9	0.73[a]
Sex (no. males)	14	9	0.20[b]
Education, years (mean ± SD)	13.9 ± 3.3	12.8 ± 2.8	0.33[a]
Cause of trauma (no. MVA)	11	8	0.42[b]
Post-resuscitation GCS (median, range)	4.5 (3–7)	3 (3–6)	**0.036**[c]
Neurosurgery	5	4	1.0[b]
ISS (no. with ISS > 25)	11	9	0.80[b]
Occurrence of secondary insults	5	12	**0.004**[b]
Days to GCS > 8 (median, range)[d]	7 (1–24)	16.5 (9–365)	**0.002**[c]
Duration of PTA, days (median, range)[d]	61.5 (23–171)	327 (39–365)	**0.0002**[c]
FIM at scan 1 (median, range)	96.5 (18–122)	20.5 (18–79)	**0.00001**[c]
DAI grade III on conventional MRI	2	7	**0.046**[b]
Contusion on conventional MRI	7	8	0.72[b]

[a]Independent-samples *t*-test; [b]Fisher's exact test; [c]Mann–Whitney U-test [d]If exceeds ~1 year follow-up, set to 365 days. Unfavourable outcome: GOS = 1–3; favourable outcome: GOS = 4–5. For significant test results (uncorrected), *P*-values are marked in bold. GOS = Glasgow outcome scale; MVA = motor vehicle accident; GCS = Glasgow coma scale; ISS = injury severity score; PTA = post-traumatic amnesia; FIM = functional independence measure; Scan 1 = initial MRI; DAI = diffuse axonal injury.

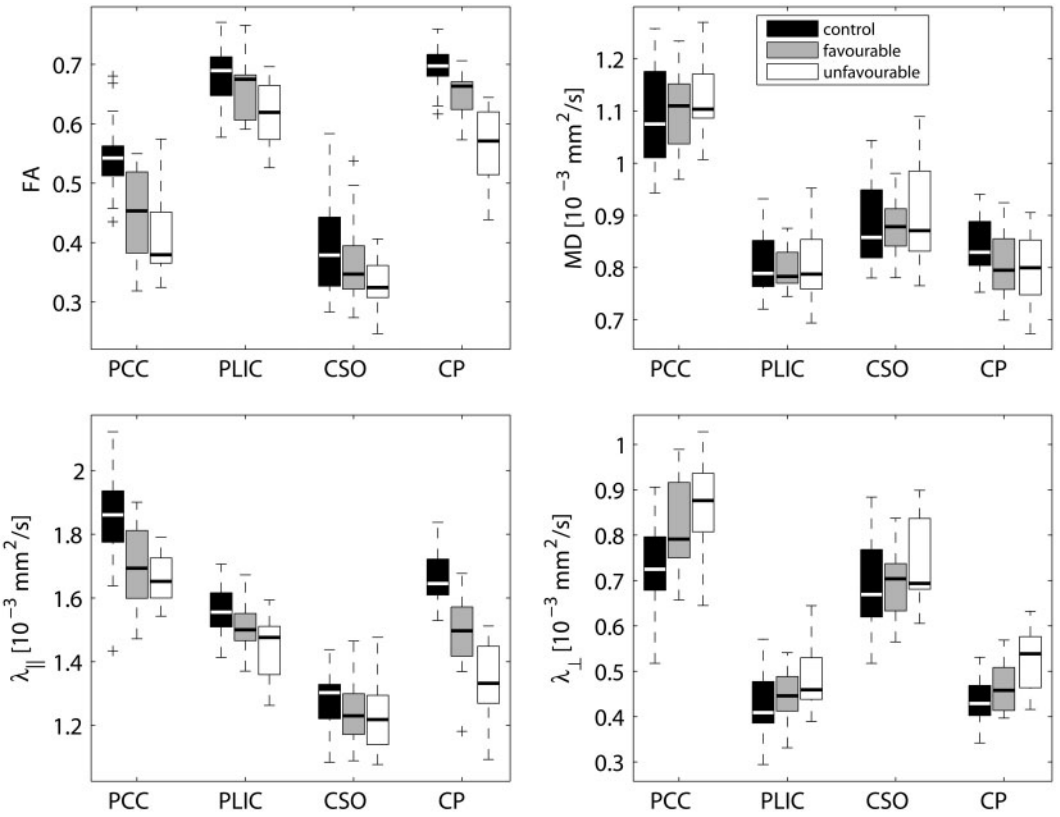

Fig. 2 Initial (~8 weeks post-injury) DTI parameters in the four white matter ROIs, grouped according to outcome at ~1 year post-injury [dichotomized GOS, unfavourable outcome: GOS = 1–3 ($n = 14$); favourable outcome: GOS = 4–5 ($n = 15$)]. Control values are shown for comparison ($n = 30$). Boxes represent lower, median (line) and upper quartiles; whiskers show the range of the data excluding outliers (+). PCC = posterior aspect of corpus callosum; PLIC = posterior limb of internal capsule; CSO = centrum semiovale; CP = cerebral peduncle.

outcome group, FA had returned to normal levels in PLIC and CSO, due to the selective interval increase of $\lambda_{\parallel}$ which in PLIC reached even supra-normal levels at follow-up ($P < 0.01$). Further analysis revealed a positive correlation between individual $\lambda_{\parallel}$ in PLIC and GOS ($r = 0.47$, $P = 0.03$, Spearman's correlation). In PCC and CP, FA remained depressed in both outcome groups, but significantly more so in patients with unfavourable outcome ($P < 0.05$ and

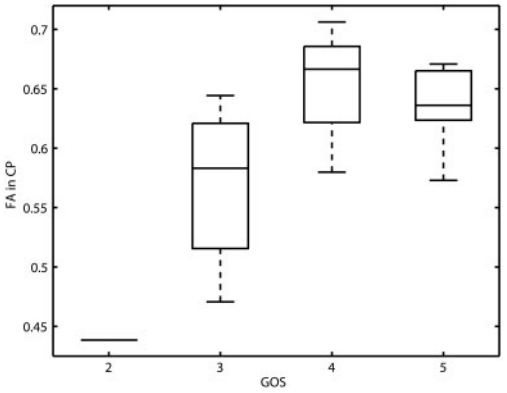

Fig. 3 Relationship between FA in the cerebral peduncle at the initial scan (~8 weeks post-injury) and 1-year outcome. Boxes represent lower, median (line) and upper quartiles; whiskers show the range of the data. Higher FA was related to better outcome ($r = 0.60$, $P < 0.001$, Spearman's correlation). GOS = Glasgow outcome scale: 1 = dead ($n = 0$), 2 = vegetative state ($n = 1$), 3 = severe disability ($n = 13$), 4 = moderate disability ($n = 9$), 5 = good recovery ($n = 6$); CP = cerebral peduncle; FA = fractional anisotropy.

$P = 0.01$, respectively). Finally, Fig. 5 displays the changes over time in favourable and unfavourable outcome patients as well as in controls.

Discussion

Using DTI, we prospectively and longitudinally examined white matter microstructure in individuals with severe TBI in the late subacute and chronic stages, and investigated the correlation to 1-year clinical outcome. In the late subacute stage (~8 weeks post-injury) we found FA to be decreased in all investigated white matter regions, due to decreased $\lambda_{\parallel}$ and increased $\lambda_{\perp}$. Patients with unfavourable 1-year outcome, according to dichotomized GOS, tended to deviate more from control DTI values than patients with favourable outcome. FA in CP at the initial scan added predictive accuracy to concomitant clinical evaluation by FIM. At follow-up DTI ~12 months post-injury, FA had normalized in PLIC and CSO, primarily in patients with favourable outcome, caused by the increase of $\lambda_{\parallel}$ to normal or supranormal levels with unchanged $\lambda_{\perp}$. In PCC and CP, $\lambda_{\parallel}$ and $\lambda_{\perp}$ both increased during the scan interval and, particularly in patients with unfavourable outcome, FA remained depressed.

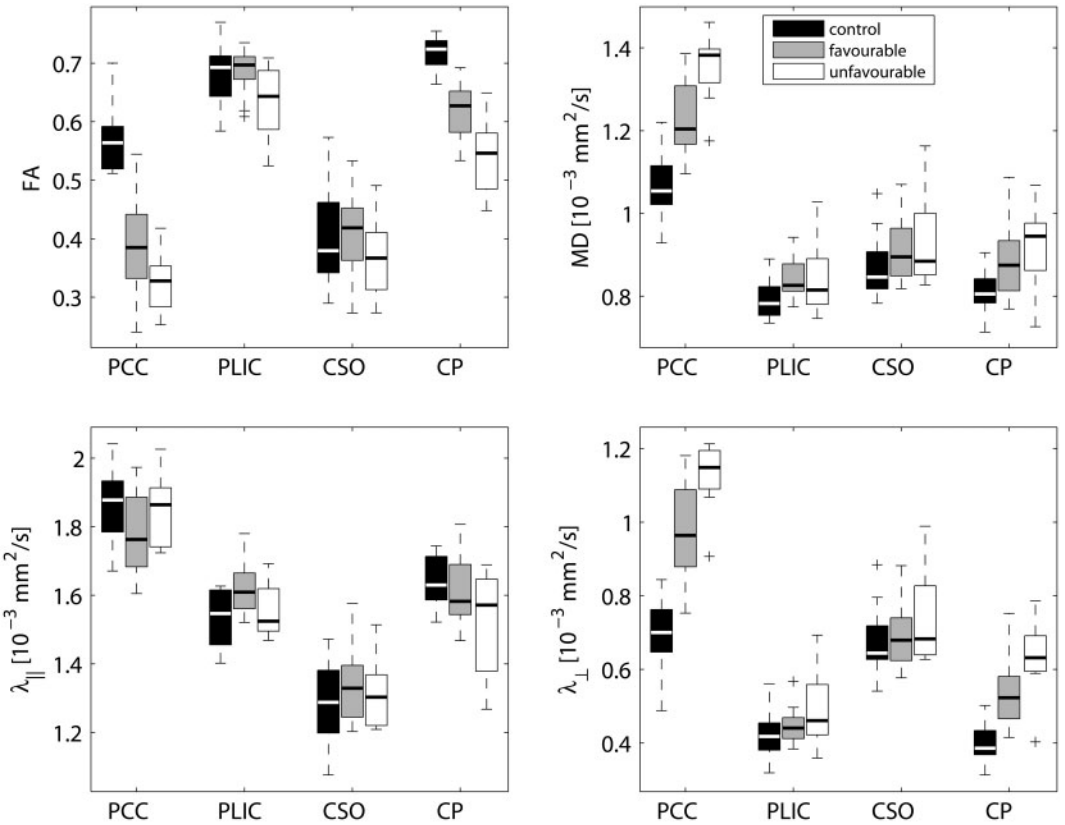

Fig. 4 Follow-up (~12 months post-injury) DTI parameters in the four white matter ROIs, grouped according to outcome at 1 year post-injury [dichotomized GOS, unfavourable outcome: GOS = 1–3 ($n = 8$); favourable outcome: GOS = 4–5 ($n = 14$)]. Control values are shown for comparison (follow-up scan, $n = 14$). Boxes represent lower, median (line) and upper quartiles; whiskers show the range of the data excluding outliers (+). PCC = posterior aspect of corpus callosum; PLIC = posterior limb of internal capsule; CSO = centrum semiovale; CP = cerebral peduncle.

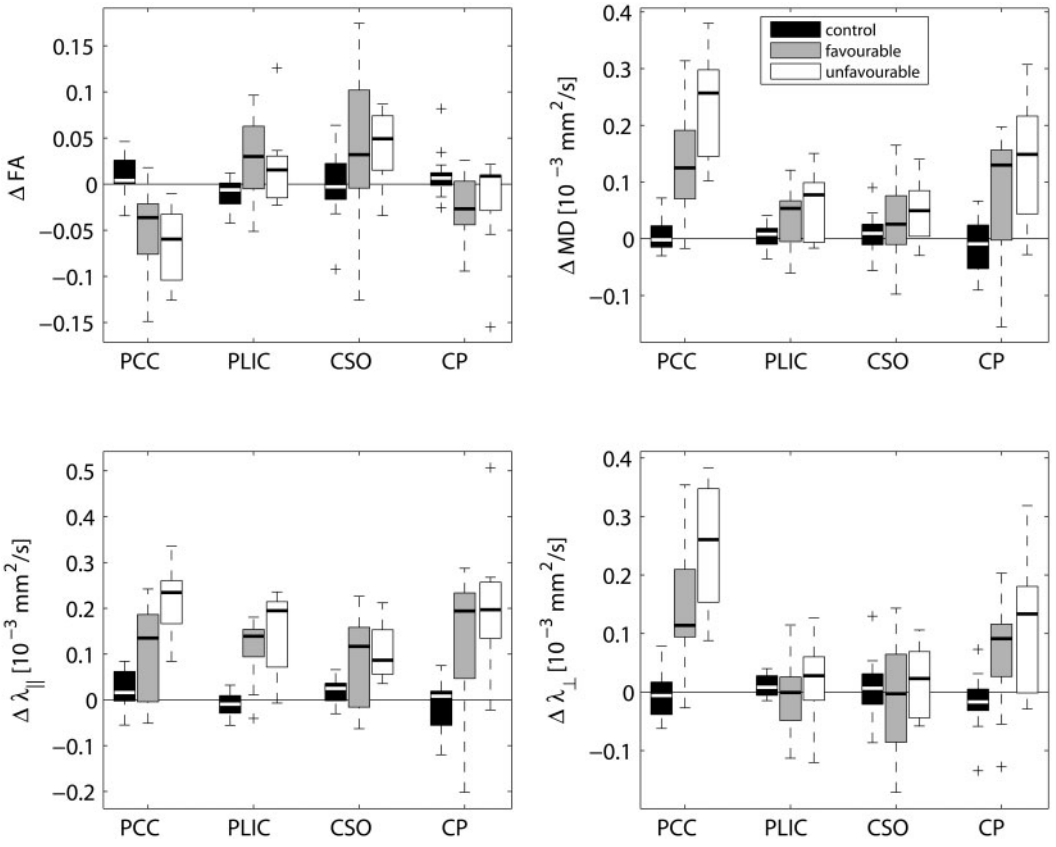

Fig. 5 Longitudinal changes (Δ = scan 2 − scan 1) of DTI parameters in the four white matter ROIs, grouped according to outcome at 1-year post-injury [dichotomized GOS, unfavourable outcome: GOS = 1–3 (n = 8); favourable outcome: GOS = 4–5 (n = 14)]. Control values are shown for comparison (follow-up scan, n = 14). Boxes represent lower, median (line) and upper quartiles; whiskers show the range of the data excluding outliers (+). PCC = posterior aspect of corpus callosum; PLIC = posterior limb of internal capsule; CSO = centrum semiovale; CP = cerebral peduncle.

Study design

The prospective longitudinal design of this study has several advantages, most importantly enabling the investigation of long-term dynamic evolution of diffusion changes, and the correlation to late clinical outcome. Serial DTI on one or two patients has previously been reported (Arfanakis *et al.*, 2002; Naganawa *et al.*, 2004; Le *et al.*, 2005; Voss *et al.*, 2006), but to our knowledge the present study is the first prospective longitudinal DTI study performed on a group of TBI patients. The study design enabled us to obtain reasonably uniform time intervals between injury-scan, scan-rescan and injury-outcome evaluation. All scans were acquired on the same scanner, and patients received a uniform intensity of rehabilitation following departmental guidelines. Furthermore, to reduce the heterogeneity inherent to clinical TBI studies, we only studied patients with severe TBI. As our patient population represented the most severely injured survivors of TBI (Engberg *et al.*, 2006), our results are however not directly comparable to those of other studies in which patients had milder or mixed injury severity. Importantly, in the present study a large proportion of the patients had sustained secondary insults.

Initial DTI and association with outcome

In the late subacute stage our findings of decreased $\lambda_{\parallel}$ and increased $\lambda_{\perp}$ in several white matter ROIs are in line with previous findings (Arfanakis *et al.*, 2002; Le *et al.*, 2005). Recently, animal models of axonal injury versus demyelination have indicated that axonal injury selectively decreases $\lambda_{\parallel}$, while demyelination increases $\lambda_{\perp}$ (Song *et al.*, 2002; Sun *et al.*, 2006). Accordingly, our results could reflect the combination of axonal injury and demyelination, but could also be the result of increased content of isotropic tissue, notably gliosis (Pierpaoli *et al.*, 2001). Regardless of the exact proportionate contribution of these pathological processes, the observed DTI pattern is consistent with Wallerian or Wallerian-like degeneration (Pierpaoli *et al.*, 2001; Thomalla *et al.*, 2004), most likely reflecting consequences of DAI and/or secondary hypoxic–ischaemic injury.

The clinical significance of the measured DTI metrics is highlighted by the correlations between these quantities and long-term functional outcome. At the initial scan, DTI parameters for patients with unfavourable outcome tended to deviate more from control values than for patients with favourable outcome. The strongest correlation with 1 year

GOS was found for FA in CP, which predicted dichotomized 1-year GOS with 76% accuracy and even added predictive accuracy to FIM evaluated at the time of the initial scan. In comparison, conventional MRI variables (e.g. DAI grade) did not add predictive information to FIM, although in this group of severely injured patients we did find a just significant association between DAI grade III and unfavourable outcome. Other studies of patients with even mild TBI have found DTI abnormalities undetected by conventional MRI (Arfanakis *et al.*, 2002; Inglese *et al.*, 2005), clearly indicating that DTI is more sensitive to traumatic white matter injury than conventional imaging. These and the present study did not, however, apply susceptibility-weighted imaging, another MRI sequence which has proven more sensitive to haemorrhagic DAI than standard T2*-weighted sequences (Tong *et al.*, 2003). To determine the prognostic value of DTI, useful in clinical practice, larger studies are clearly needed.

Longitudinal findings—microstructural reorganization?

The 1-year follow-up DTI of 22 of the patients and 14 of the controls revealed interesting changes in the patients during a period of time when the vast majority of them improved considerably in function (median FIM increased from 48 to 113 during the scan interval). If we assume that the observed increase of $\lambda_{\parallel}$ in various white matter regions does reflect true alterations of tissue microstructure over time, which processes might underlie these late DTI changes? In PCC and CP, the increase of all eigenvalues over time most likely represents accumulation of extracellular fluid as a consequence of progressive structural degradation. In PCC, DAI-related lesions were visible on conventional MRI in the majority of patients, and it may be that with time the filling of cystic spaces by CSF contributes to these alterations. In PLIC and CSO, however, the observed interval increase of $\lambda_{\parallel}$ was not accompanied by an increase of $\lambda_{\perp}$, and so is unlikely to represent a change in extracellular fluid content. In the vast majority of patients the tissue comprised by these ROIs was normal-appearing on conventional MRI.

The changes in CSO should be interpreted with caution because of the limitations of the tensor model in this complex region (see next section). However, the fact that a similar pattern of DTI changes over time was found in the highly homogeneous PLIC argues in favour of true microstructural alterations. One possible interpretation of this interesting finding is that, despite progressive general atrophy, some reorganization of tissue microstructure has taken place during the scan interval. Specifically, late axonal recovery or even axonal regrowth (without concomitant remyelination) could account for the selective increase of $\lambda_{\parallel}$ and the resulting FA increase. In a recent report including data on one patient who emerged from a minimally conscious state as late as 19 years post-trauma, the authors found what was interpreted as a transient increase of FA in the cuneus–precuneus area, followed by an FA increase in the cerebellar vermis (Voss *et al.*, 2006). Our findings point towards an inference similar to that suggested by Voss and coauthors, namely that the observed FA increase over time may represent axonal regrowth at late stages following severe TBI. An increasing body of evidence points towards the role of neuroplastic changes as underlying late recovery following TBI (for a review, see Levin, 2003), and our study supports the notion that DTI may serve to probe white matter regeneration *in vivo*. To map the exact brain areas involved in white matter reorganization, future voxel-based analyses of longitudinal DTI data are needed. Using a voxel-based approach one could also investigate whether some relationship exists between DTI changes and brain volume changes over time. However, a major challenge to voxel-based analysis of DTI data is the registration of fibre tracts between mutually heterogeneous brains.

Limitations and possible pitfalls

Brains that structurally change over time pose certain challenges to the interpretation of longitudinal DTI findings. The tensor model is unable to model multiple fibre populations within each voxel, and specifically in complex regions of crossing fibre populations this is an important limitation. For instance, the perpendicular crossing within one voxel of two highly anisotropic fibre populations will lead to a low FA measured in that voxel. If one of these fibre populations degenerates over time, the orientational coherence within the voxel, and hence FA, increases. This major limitation of the tensor model demands cautious interpretation of longitudinal DTI findings in complex regions where fibres intersect, such as the CSO. In this study FA maps did reveal clear inhomogeneities within the CSO that appeared homogeneous on conventional MRI. Therefore we cannot exclude the possibility that the observed increase of FA over time in CSO could be caused by degeneration of one fibre population e.g. of fibres stemming from the corpus callosum. In contrast, the other white matter ROIs, PCC, PLIC and CP are thought to consist of well-defined coherently oriented fibre bundles. This was also suggested by the high control FA values in these ROIs (Table 3) and homogeneous appearance on FA maps. For these reasons we consider it unlikely that this limitation of the tensor model would account for our findings in these regions. Future studies, using more advanced diffusion imaging techniques such as q-ball imaging (Tuch, 2004), may allow modelling of different fibre populations within each voxel.

One important issue, which has already been dealt with, is that of systematic differences in partial voluming. Corpus callosum is particularly prone to partial voluming from neighbouring CSF, and even more so when DTI voxels are larger in the *z*-direction. As a consequence of progressive callosal thinning following DAI one could anticipate

increased partial voluming in patients, particularly at follow-up. Our results following successive erosion of the PCC could indicate partial voluming of the original ROI. However, differences between patients and controls as well as longitudinal changes remained significant following extensive erosion. As opposed to PCC, which was defined (except anteriorly) by its anatomical borders, the other ROIs were kept distant from neighbouring tissue. Although partial voluming cannot be avoided completely, the anatomical orientation of these ROIs relative to the *z*-direction makes them less susceptible to major influence by partial volume effects.

Systematic group or time differences in data acquisition need to be considered. In the present study, patients and controls were scanned interleaved, and with a similar scan–rescan interval. As we found no trends towards any time effects in the control group, any major influence of scanner drift on our results is considered highly unlikely.

Most patients ($n = 25$) needed sedation for the initial scan, while only a few ($n = 4$) were sedated for the follow-up scan. The potential influence of propofol sedation on parameters measured by DTI has not been systematically investigated. While any direct effect on tissue microstructure seems theoretically implausible, an indirect effect e.g. through change of body temperature could influence all diffusivities in the same direction. However, a temperature change of more than 8°C would be required to account for the observed changes of up to 20% in the eigenvalues [the diffusion coefficient varies ~2.4%/°C in the physiological temperature range (Le Bihan, 1995)], and obviously, this cannot have occurred. Furthermore, systematic differences between sedated versus non-sedated individuals regarding noise due to motion might cause differential introduction of errors in the tensor computation (Chang *et al.*, 2005). However, we found no tendency towards systematic differences in the DTI parameters measured in sedated versus non-sedated patients. Moreover, diffusivities measured in CSF did not tend to differ between patients and controls or between initial and follow-up scans. This argues against any major confounding of our results by factors related to sedation.

One final limitation of our study relates to the clinical scales used. It would have been desirable to compare individual DTI changes and degree of functional improvement during the scan interval. However, as the distribution of FIM values at follow-up suffered from ceiling effects, this scale did not allow for adequate investigation of such a possible relationship. The Disability Rating Scale (Rappaport *et al.*, 1982) (range 0–29) may have offered less susceptibility to ceiling effects, however this would have been at the expense of reduced sensitivity to the subtle, yet sometimes significant, changes in function within a limited window of recovery. Monitoring clinical progress and outcome in TBI patients is a general and complex problem with a difficult choice between using a set of detailed scales that are consecutively applied as recovery proceeds, and a single, yet less detailed scale that covers all phases of recovery.

Conclusions

This prospective longitudinal study of severe TBI provides new insight into the evolution of DTI parameters during rehabilitation, and suggests clinical relevance of these quantities to long-term clinical outcome. Our findings indicate microstructural alterations during the chronic stage of severe TBI, which may represent structural reorganization relevant to clinical recovery. DTI non-invasively provides quantitative pathophysiological information *in vivo*, and the prospect of tracking white matter microstructural changes over time holds the promise of measuring neuroplasticity and repair following TBI, which eventually may offer a way of monitoring therapeutic response. Future longitudinal studies are warranted that combine DTI with volumetric measurements and with other MRI modalities, such as spectroscopy, ideally with multiple data acquisitions at shorter time intervals. The potential of DTI as a prognostic marker needs further investigation in larger studies.

Acknowledgements

The authors would like to thank the participants of this study, Henrik K. Mathiesen and Sussi Larsen for skilled MRI acquisition, Hanns Reich for expert anaesthesiological assistance, Klaus Larsen and Kristoffer H. Madsen for statistical help, Arnold Skimminge and Tim Dyrby for advice on data analysis, and the staff at the Brain Injury Unit for experienced clinical rating. This study was supported by a generous grant from the Elsass Foundation.

References

Arfanakis K, Haughton VM, Carew JD, Rogers BP, Dempsey RJ, Meyerand ME. Diffusion tensor MR imaging in diffuse axonal injury. Am J Neuroradiol 2002; 23: 794–802.

Basser PJ, Mattiello J, Le Bihan D. MR diffusion tensor spectroscopy and imaging. Biophys J 1994; 66: 259–67.

Chan JH, Tsui EY, Peh WC, Fong D, Fok KF, Leung KM, et al. Diffuse axonal injury: detection of changes in anisotropy of water diffusion by diffusion-weighted imaging. Neuroradiology 2003; 45: 34–8.

Chang LC, Jones DK, Pierpaoli C. RESTORE: robust estimation of tensors by outlier rejection. Magn Reson Med 2005; 53: 1088–95.

Chesnut RM, Marshall LF, Klauber MR, Blunt BA, Baldwin N, Eisenberg HM, et al. The role of secondary brain injury in determining outcome from severe head injury. J Trauma 1993; 34: 216–22.

Choi SC, Clifton GL, Marmarou A, Miller ER. Misclassification and treatment effect on primary outcome measures in clinical trials of severe neurotrauma. J Neurotrauma 2002; 19: 17–22.

Engberg AW, Liebach A, Nordenbo A. Centralized rehabilitation after severe traumatic brain injury – a population-based study. Acta Neurol Scand 2006; 113: 178–84.

Gentry LR. Head trauma. In: Atlas SW, editor. Magnetic resonance imaging of the brain and spine. 3rd edn., Philadelphia: Lippincott Williams & Wilkins; 2002. p. 1059–98.

Graham DI, Gennarelli TA. Trauma. In: Graham DI, Lantos PL, editors. Greenfield's neuropathology. 6th edn., London: Arnold; 1997. p. 197–262.

Granger CV, Hamilton BB, Keith RA, Zielesny M, Sherwin FS. Advances in functional assessment for medical rehabilitation. Top Geriatr Rehabil 1986; 1: 59–74.

Greenspan L, McLellan BA, Greig H. Abbreviated Injury Scale and Injury Severity Score: a scoring chart. J Trauma 1985; 25: 60–4.

Huisman TA, Schwamm LH, Schaefer PW, Koroshetz WJ, Shetty-Alva N, Ozsunar Y, et al. Diffusion tensor imaging as potential biomarker of white matter injury in diffuse axonal injury. Am J Neuroradiol 2004; 25: 370–6.

Inglese M, Makani S, Johnson G, Cohen BA, Silver JA, Gonen O, et al. Diffuse axonal injury in mild traumatic brain injury: a diffusion tensor imaging study. J Neurosurg 2005; 103: 298–303.

Jennett B, Bond M. Assessment of outcome after severe brain damage. Lancet 1975; 1: 480–4.

Jones PA, Andrews PJ, Midgley S, Anderson SI, Piper IR, Tocher JL, et al. Measuring the burden of secondary insults in head-injured patients during intensive care. J Neurosurg Anesthesiol 1994; 6: 4–14.

Le Bihan D. Temperature imaging by NMR. In: Le Bihan D, editor. Diffusion and perfusion magnetic resonance imaging. Applications to functional MRI. New York: Raven Press; 1995. p. 181–7.

Le TH, Mukherjee P, Henry RG, Berman JI, Ware M, Manley GT. Diffusion tensor imaging with three-dimensional fiber tractography of traumatic axonal shearing injury: an imaging correlate for the posterior callosal ''disconnection'' syndrome: case report. Neurosurgery 2005; 56: 189.

Levin HS. Neuroplasticity following non-penetrating traumatic brain injury. Brain Inj 2003; 17: 665–74.

Levin HS, O'Donnell VM, Grossman RG. The Galveston Orientation and Amnesia Test. A practical scale to assess cognition after head injury. J Nerv Ment Dis 1979; 167: 675–84.

Mac Donald CL, Dikranian K, Song SK, Bayly PV, Holtzman DM, Brody DL. Detection of traumatic axonal injury with diffusion tensor imaging in a mouse model of traumatic brain injury. Exp Neurol 2007; 205: 116–31.

MacKenzie EJ. Epidemiology of injuries: current trends and future challenges. Epidemiol Rev 2000; 22: 112–9.

Marenco S, Rawlings R, Rohde GK, Barnett AS, Honea RA, Pierpaoli C, et al. Regional distribution of measurement error in diffusion tensor imaging. Psychiatry Res 2006; 147: 69–78.

Naganawa S, Sato C, Ishihra S, Kumada H, Ishigaki T, Miura S, et al. Serial evaluation of diffusion tensor brain fiber tracking in a patient with severe diffuse axonal injury. Am J Neuroradiol 2004; 25: 1553–6.

Nakayama N, Okumura A, Shinoda J, Yasokawa YT, Miwa K, Yoshimura SI, et al. Evidence for white matter disruption in traumatic brain injury without macroscopic lesions. J Neurol Neurosurg Psychiatry 2006; 77: 850–5.

Pierpaoli C, Basser PJ. Toward a quantitative assessment of diffusion anisotropy. Magn Reson Med 1996; 36: 893–906.

Pierpaoli C, Jezzard P, Basser PJ, Barnett A, Di Chiro G. Diffusion tensor MR imaging of the human brain. Radiology 1996; 201: 637–48.

Pierpaoli C, Barnett A, Pajevic S, Chen R, Penix L, Virta A, et al. Water diffusion changes in Wallerian degeneration and their dependence on white matter architecture. Neuroimage 2001; 13: 1174–85.

Ptak T, Sheridan RL, Rhea JT, Gervasini AA, Yun JH, Curran MA, et al. Cerebral fractional anisotropy score in trauma patients: a new indicator of white matter injury after trauma. Am J Radiol 2003; 181: 1401–7.

Rappaport M, Hall KM, Hopkins K, Belleza T, Cope DN. Disability rating scale for severe head trauma: coma to community. Arch Phys Med Rehabil 1982; 63: 118–23.

Rugg-Gunn FJ, Symms MR, Barker GJ, Greenwood R, Duncan JS. Diffusion imaging shows abnormalities after blunt head trauma when conventional magnetic resonance imaging is normal. J Neurol Neurosurg Psychiatry 2001; 70: 530–3.

Salmond CH, Menon DK, Chatfield DA, Williams GB, Pena A, Sahakian BJ, et al. Diffusion tensor imaging in chronic head injury survivors: correlations with learning and memory indices. Neuroimage 2006; 29: 117–24.

Schiff ND. Multimodal neuroimaging approaches to disorders of consciousness. J Head Trauma Rehabil 2006; 21: 388–97.

Song SK, Sun SW, Ramsbottom MJ, Change C, Russell J, Cross AH. Dysmyelination revealed through MRI as increased radial (but unchanged axial) diffusion of water. Neuroimage 2002; 17: 1429–36.

Sun SW, Liang HF, Trinkaus K, Cross AH, Armstrong RC, Song SK. Noninvasive detection of cuprizone induced axonal damage and demyelination in the mouse corpus callosum. Magn Reson Med 2006; 55: 302–8.

Teasdale G, Jennett B. Assessment of coma and impaired consciousness. A practical scale. Lancet 1974; 2: 81–4.

Thomalla G, Glauche V, Koch MA, Beaulieu C, Weiller C, Rother J. Diffusion tensor imaging detects early Wallerian degeneration of the pyramidal tract after ischemic stroke. Neuroimage 2004; 22: 1767–74.

Tong KA, Ashwal S, Holshouser BA, Shutter LA, Herigault G, Haacke EM, et al. Hemorrhagic shearing lesions in children and adolescents with posttraumatic diffuse axonal injury: improved detection and initial results. Radiology 2003; 227: 332–9.

Tuch DS. Q-ball imaging. Magn Reson Med 2004; 52: 1358–72.

Voss HU, Uluc AM, Dyke JP, Watts R, Kobylarz EJ, McCandliss BD, et al. Possible axonal regrowth in late recovery from the minimally conscious state. J Clin Invest 2006; 116: 2005–11.